ORIGINAL ARTICLE

Novel (*Z*)/(*E*)-1,2,4-triazole derivatives containing oxime ether moiety as potential ergosterol biosynthesis inhibitors: design, preparation, antifungal evaluation, and molecular docking

Shengxin Sun[1] · Jinghua Yan[1] · Lang Tai[1] · Jianqi Chai[1,2] · Haoran Hu[1] · Ling Han[1] · Aimin Lu[1,2] · Chunlong Yang[1,2] · Min Chen[1,2]

Abstract

Inspired by the highly effective and broad-spectrum antifungal activity of ergosterol biosynthesis inhibitions, a series of novel 1,2,4-triazole derivatives containing oxime ether moiety were constructed for screening the bioactivity against phytopathogenic fungi. The (*Z*)- and (*E*)-isomers of target compounds were successfully separated and identified by the spectroscopy and single crystal X-ray diffraction analyses. The bioassay results showed that the (*Z*)-isomers of target compounds possessed higher antifungal activity than the (*E*)-isomers. Strikingly, the compound (*Z*)-**5o** exhibited excellent antifungal activity against *Rhizoctonia solani* with the EC_{50} value of 0.41 µg/mL in vitro and preventive effect of 94.58% in vivo at 200 µg/mL, which was comparable to the positive control tebuconazole. The scanning electron microscopy observation indicated that the compound (*Z*)-**5o** caused the mycelial morphology to become wizened and wrinkled. The molecular docking modes of (*Z*)-**5o** and (*E*)-**5o** with the potential target protein *Rs*CYP51 were especially compared. And the main interactions between ligands and amino acid residues were carefully analyzed to preliminarily explain the mechanism leading to the difference of activity between two isomers. The study provided a new lead molecular skeleton for developing novel triazole fungicides targeting ergosterol biosynthesis.
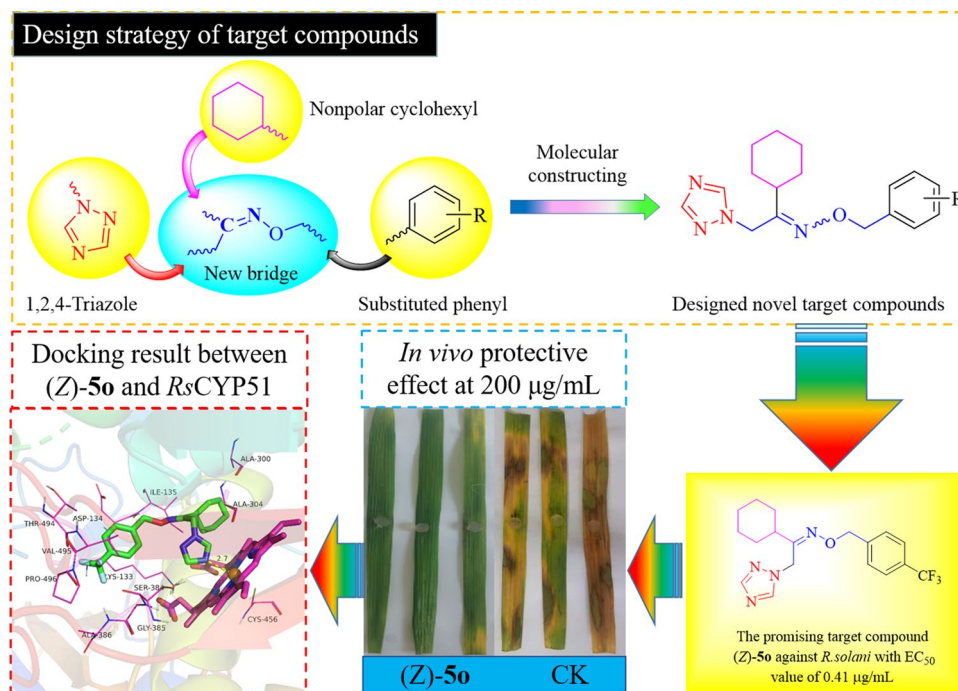
✉ Chunlong Yang
    ycl@njau.edu.cn

✉ Min Chen
    chenmin@njau.edu.cn

1   College of Sciences, Nanjing Agricultural University, Nanjing 210095, China

2   Jiangsu Key Laboratory of Pesticide Science, Nanjing Agricultural University, Nanjing 210095, China

Graphical abstract

Keywords 1,2,4-Triazole · Oxime ether · Antifungal activity · Molecular docking

Introduction

Phytopathogenic fungi have become the culprits of food

safety and agricultural yield reductions [1, 2]. As the vital method to effectively control phytopathogenic fungi, agricultural fungicides should not only equip with highly
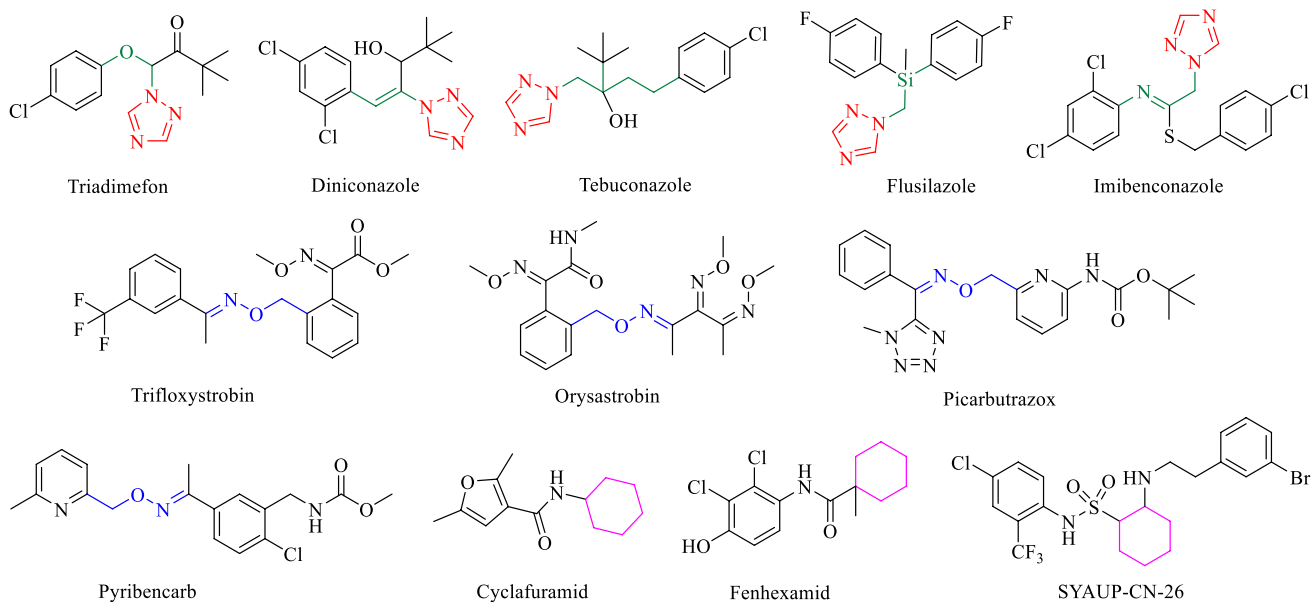

Fig. 1 Agricultural fungicides containing a triazole, oxime ether or cyclohexyl fragment

effective bioactivities, but also possess the unique capability to distinguish fungi from plants and animals. Ergosterol plays an important role in mediating the permeability and fluidity of fungi cell membranes, and is structurally different from those sterols contained in animals and plants [3–5]. The lanosterol 14α-demethylase (coded by CYP51) belonging to a cytochrome P450 catalyzes the biosynthesis of ergosterol that maintains the integrity and rigidity of fungal cell membranes [3, 6]. Once the above ergosterol biosynthesis is hindered, fungal cell membranes will be speedily destructed, which finally result in the inhibition or death of phytopathogenic fungi [7]. During the last three decades, the distinctive function of CYP51 inspired the development of demethylation inhibitors (DMIs) that feature broad-spectrum bioactivities, convenient syntheses and affordable prices [8]. Triadimefon (Fig. 1) featuring strong systemic absorption and persistence was developed as the DMI fungicide that mainly used in controlling powdery mildew, rust and loose smut [9]. Subsequently, numerous antifungal molecules were successively developed as the commercialized DMIs with high efficiency, low toxicity and broad-spectrum properties, such as diniconazole, tebuconazole, flusilazole and imibenconazole [10–12]. These DMI fungicides mentioned-above tend to have some common structural features that were described below. One structural feature could be expressed as the introduction of benzene ring and 1,2,4-triazole fragments. Another is the presence of a special bridge that used to link the benzene ring and 1,2,4-triazole fragments, such as ether chain (triadimefon), alkene chain (diniconazole), alkyl chain (tebuconazole), silyl linkage (flusilazole) and Schiff base bridge (imibenconazole) (Fig. 1). A large number of publications have indicated that altering the bridge group in DMIs is one of the important ways to develop new compounds with high antifungal activity [3, 13, 14].

Oxime ethers are the highly effective and low toxicity fragments that were widely used in the development of anticancer, bactericides, herbicides, fungicides, viricides and insecticides, and have occupied a more important position in fungicides [13–20]. In 1974, DuPont successfully developed the first oxime ether fungicide cymoxanil that mainly used to control downy mildew and late blight [21]. Subsequently, oxime ether fungicides were developed rapidly. During 1995–2003, a series of methoxyacrylate fungicides containing an oxime ether fragment as the bridge group, such as trifloxystrobin, orysastrobin, enostroburin and fenaminostrobin, were discovered successively. Due to their unique mechanism of action and environmental friendliness, more attention was paid to the development of oxime ether fungicides [22]. Some other commercialized fungicides containing a oxime ether bridge structure, such as picarbutrazox and pyribencarb, were also disclosed to protect excellently tomatoes, rice, soybeans and other crops from a range of pathogenic fungi [23–25]. Latterly, the researchers reported that the derivatives containing an oxime ether as a bridge group possessed better bioactivity than those containing an amide bridge in succinate dehydrogenase inhibitors (SDHIs) and other bridges in many other compounds by molecule docking [26]. These evidences persuaded us to choose the oxime ether as a bridge group to design new triazole compounds.

In order to search novel lead molecules of ergosterol biosynthesis inhibitions (DMIs), the oxime ether fragment was used to bridge the 1,2,4-triazole and substituted phenyl groups to construct the basic target molecular skeleton (Fig. 2). The cyclohexyl group considered as a typical hydrophobic group has effectively improved the lipophilicity of some fungicides, such as cyclafuramid, fenhexamid and SYAUP-CN-26 [27–29], and was introduced into the bridge segment of the target molecules. The designed compounds were synthesized and separated by the column chromatography to obtain corresponding (Z)-isomers and (E)-isomers, which were, respectively, evaluated for the bioactivity in vitro against phytopathogenic fungi. The highly active compound (Z)-5o was selected to determine the antifungal activity in vivo and the effect on mycelial cell morphology. Moreover, the two isomers (Z)-5o and (E)-5o were, respectively, docked with the potential target protein RsCYP51, a homology model was constructed by the amino
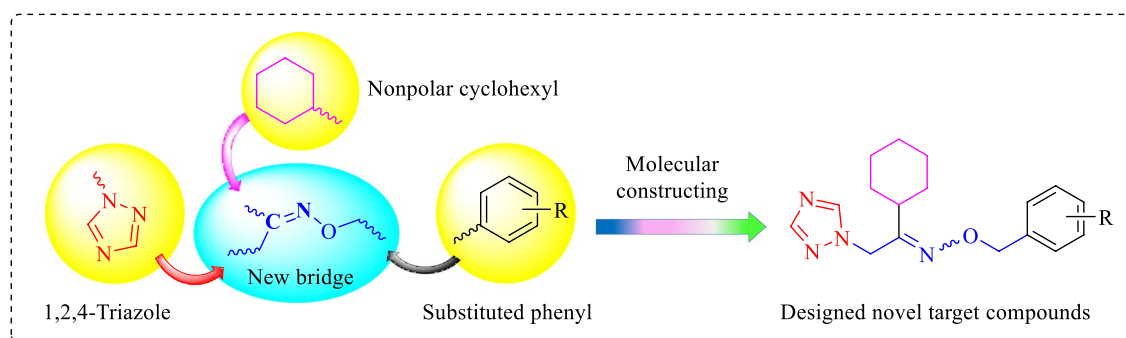

Fig. 2 Design strategy of target compounds as novel fungicides

acid sequences of *Rhizoctonia solani* and selected the protein CYP51 (PDB code: 4UHL) as template. The molecular docking results preliminarily explaining the mechanism leading to the difference of antifungal activity.
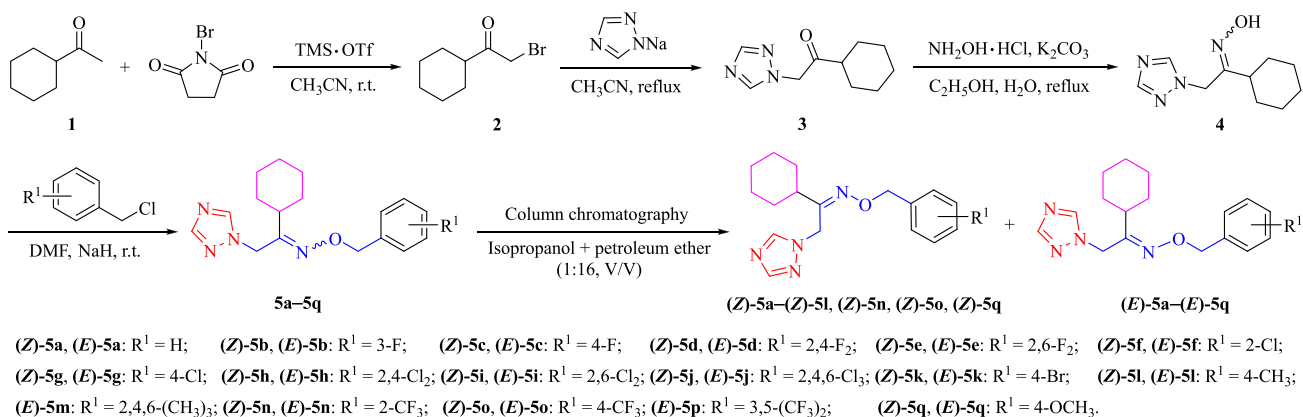
Results and discussion

Preparation of target compounds

The synthesis route of designed target compounds, i.e., 1,2,4-triazole derivatives containing the oxime ether and cyclohexyl fragments as potential ergosterol biosynthesis inhibitors, together with the separation way of (*Z*)/(*E*)-isomers were shown in Scheme 1 [15, 30, 31]. As the mixtures of two isomers, the target products **5a–5q** were synthesized by four steps of bromination, triazole substitution, oximation and oxime etherification. The first intermediate 2-bromo-1-cyclohexylethan-1-one **2** was obtained by the reaction of starting material 1-cyclohexylethan-1-one **1** with the bromination reagent *N*-bromosuccinimide (NBS) in the presence of trimethylsilyl trifluoromethanesulfonate (TMS·OTf) as the initiator. The compound **2** was reacted with sodium 1,2,4-triazole to conveniently synthesize the intermediate

1-cyclohexyl-2-(1*H*-1,2,4-triazol-1-yl) ethan-1-one **3**, which was oximated by hydroxylamine hydrochloride with potassium carbonate as the acid binding agent to generate the crucial intermediate 1-cyclohexyl-2-(1*H*-1,2,4-triazol-1-yl) ethan-1-one oxime **4**. Then, different substituted benzyl chlorides were, respectively, reacted with the compound **4** to give the target compounds **5a–5q**, which were further separated by silica gel column chromatography to contribute the (*Z*)-isomers of (*Z*)-**5a**–(*Z*)-**5l**, (*Z*)-**5n**, (*Z*)-**5o**, and (*Z*)-**5q**, and (*E*)-isomers of (*E*)-**5a**–(*E*)-**5q**.

Structural characterization of target compounds

All the prepared target compounds including 15 (*Z*)-isomers and 17 (*E*)-isomers were characterized, respectively, by ^{1}H-NMR, ^{13}C-NMR, and HRMS spectra. Some compounds containing fluorine atom were confirmed by ^{19}F-NMR spectrum. The collected spectral data were consistent with the target molecules. Furthermore, the compound (*E*)-**5h** was deeply analyzed as a typical example using the single crystal X-ray diffraction. As a solid, the compound (*E*)-**5h** was dissolved in a mixed solution of dimethyl sulfoxide and methanol (V:V = 1:3). After slow volatilization at room temperature, a colorless transparent crystal was obtained. The

(*Z*)-**5a**, (*E*)-**5a**: R^1 = H;   (*Z*)-**5b**, (*E*)-**5b**: R^1 = 3-F;   (*Z*)-**5c**, (*E*)-**5c**: R^1 = 4-F;   (*Z*)-**5d**, (*E*)-**5d**: R^1 = 2,4-F$_2$;   (*Z*)-**5e**, (*E*)-**5e**: R^1 = 2,6-F$_2$;   (*Z*)-**5f**, (*E*)-**5f**: R^1 = 2-Cl;

(*Z*)-**5g**, (*E*)-**5g**: R^1 = 4-Cl;   (*Z*)-**5h**, (*E*)-**5h**: R^1 = 2,4-Cl$_2$;   (*Z*)-**5i**, (*E*)-**5i**: R^1 = 2,6-Cl$_2$;   (*Z*)-**5j**, (*E*)-**5j**: R^1 = 2,4,6-Cl$_3$;   (*Z*)-**5k**, (*E*)-**5k**: R^1 = 4-Br;   (*Z*)-**5l**, (*E*)-**5l**: R^1 = 4-CH$_3$;

(*E*)-**5m**: R^1 = 2,4,6-(CH$_3$)$_3$;   (*Z*)-**5n**, (*E*)-**5n**: R^1 = 2-CF$_3$;   (*Z*)-**5o**, (*E*)-**5o**: R^1 = 4-CF$_3$;   (*E*)-**5p**: R^1 = 3,5-(CF$_3$)$_2$;   (*Z*)-**5q**, (*E*)-**5q**: R^1 = 4-OCH$_3$.

Scheme 1 Preparation route of designed target compounds

Fig. 3 Molecular ellipsoid diagram (**A**) and crystal packing diagram (**B**) of target compound (*E*)-**5h**. Red dashed lines show hydrogen bonds (CCDC number: 2102936)
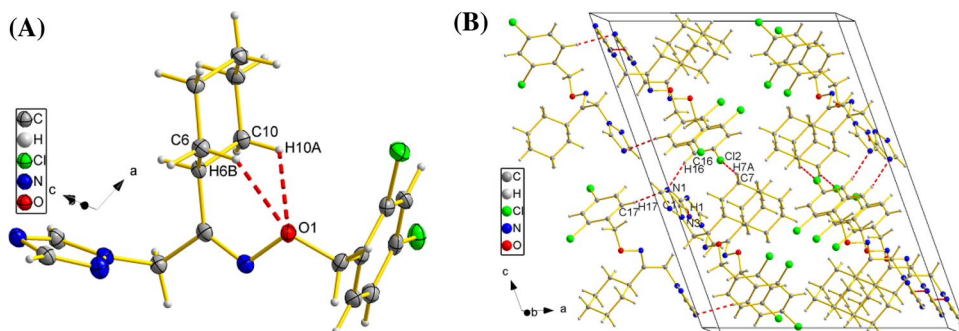
crystal diffraction data were collected and analyzed by the reported methods [32]. The compound (*E*)-**5h** crystallized in the monoclinic, space group $P2_1/c$. The corresponding crystal structure diagram and crystal packing diagram are shown in Fig. 3A, B.

In vitro antifungal activity

In vitro antifungal activities of target compounds were determined against *Rhizoctonia solani* (*R. solani*),

Fusarium graminearum (*F. graminearum*), *Botrytis cinerea* (*B. cinerea*), and *Alternaria solani* (*A. solani*) at 50 µg/mL by a typical mycelial growth rate method [33, 34]. As shown in Table 1, the bioassay data indicated that the constructed target compounds selectively possessed dramatic antifungal effects against *R. solani*, *F. graminearum*, and *B. cinerea*. Firstly, the inhibitory rates of the target compounds against *R. solani* were between 53.6% and 90.9%, which were all superior to that of the control fungicide hymexazol (49.4%). Among which the

Table 1 Inhibitory rates (%) of target compounds against four phytopathogenic fungi at 50 µg/mL

Compound	R^1	*R. solani*	*F. graminearum*	*B. cinerea*	*A. solani*
(*Z*)-**5a**	H	83.3 ± 0.3	53.8 ± 1.7	32.7 ± 0.3	14.2 ± 0.2
(*E*)-**5a**	H	75.9 ± 0.7	47.2 ± 0.6	30.1 ± 0.6	7.0 ± 0.3
(*Z*)-**5b**	3-F	79.7 ± 0.9	58.2 ± 0.8	40.6 ± 0.4	19.3 ± 0.2
(*E*)-**5b**	3-F	70.5 ± 0.3	54.3 ± 0.7	32.3 ± 0.8	22.2 ± 0.3
(*Z*)-**5c**	4-F	86.5 ± 0.3	55.6 ± 1.0	50.1 ± 0.7	10.5 ± 1.0
(*E*)-**5c**	4-F	76.4 ± 0.9	60.9 ± 0.5	54.6 ± 0.5	16.9 ± 0.3
(*Z*)-**5d**	2,4-F_2	85.7 ± 0.1	56.3 ± 1.1	43.3 ± 0.8	10.2 ± 0.7
(*E*)-**5d**	2,4-F_2	77.5 ± 0.3	48.1 ± 0.7	46.3 ± 0.8	8.2 ± 0.6
(*Z*)-**5e**	2,6-F_2	79.1 ± 0.4	67.3 ± 0.3	46.5 ± 1.8	15.7 ± 0.6
(*E*)-**5e**	2,6-F_2	81.2 ± 1.6	50.7 ± 0.1	50.5 ± 1.5	13.4 ± 0.4
(*Z*)-**5f**	2-Cl	86.9 ± 0.2	57.2 ± 0.5	48.5 ± 1.0	9.8 ± 0.5
(*E*)-**5f**	2-Cl	84.6 ± 0.4	59.9 ± 0.8	65.8 ± 0.4	19.3 ± 0.8
(*Z*)-**5g**	4-Cl	85.0 ± 0.6	65.9 ± 0.8	53.8 ± 0.6	13.6 ± 0.6
(*E*)-**5g**	4-Cl	85.4 ± 0.3	73.8 ± 0.4	60.5 ± 0.6	23.3 ± 0.4
(*Z*)-**5h**	2,4-Cl_2	78.1 ± 1.1	62.5 ± 1.1	49.6 ± 0.5	22.5 ± 1.1
(*E*)-**5h**	2,4-Cl_2	87.6 ± 0.4	72.4 ± 0.4	63.7 ± 0.6	24.0 ± 0.3
(*Z*)-**5i**	2,6-Cl_2	80.6 ± 0.4	64.0 ± 0.3	54.8 ± 0.5	16.0 ± 1.8
(*E*)-**5i**	2,6-Cl_2	78.5 ± 0.6	61.9 ± 0.5	68.5 ± 0.3	19.9 ± 0.7
(*Z*)-**5j**	2,4,6-Cl_3	89.0 ± 0.4	59.1 ± 1.9	55.0 ± 0.6	20.3 ± 1.2
(*E*)-**5j**	2,4,6-Cl_3	81.9 ± 2.5	45.3 ± 0.8	65.4 ± 0.6	20.8 ± 2.1
(*Z*)-**5k**	4-Br	84.2 ± 0.8	66.9 ± 0.5	43.6 ± 0.5	6.3 ± 0.5
(*E*)-**5k**	4-Br	83.5 ± 0.3	73.0 ± 0.2	58.6 ± 0.6	13.0 ± 1.2
(*Z*)-**5l**	4-CH_3	82.9 ± 0.8	65.3 ± 0.6	48.6 ± 0.4	7.6 ± 2.1
(*E*)-**5l**	4-CH_3	83.5 ± 0.7	67.5 ± 0.6	59.8 ± 1.0	8.9 ± 0.6
(*E*)-**5m**	2,4,6-$(CH_3)_3$	84.3 ± 0.3	76.8 ± 0.2	69.4 ± 1.0	14.2 ± 0.3
(*Z*)-**5n**	2-CF_3	85.6 ± 0.4	65.9 ± 0.4	39.6 ± 0.8	13.1 ± 0.3
(*E*)-**5n**	2-CF_3	84.8 ± 0.5	53.6 ± 0.3	49.0 ± 0.8	11.4 ± 0.3
(*Z*)-**5o**	4-CF_3	90.9 ± 0.4	68.2 ± 0.6	53.6 ± 0.5	26.3 ± 0.6
(*E*)-**5o**	4-CF_3	89.7 ± 0.3	53.0 ± 0.8	62.8 ± 1.3	10.0 ± 0.8
(*E*)-**5p**	3,5-$(CF_3)_2$	84.4 ± 0.8	89.1 ± 0.8	71.9 ± 0.4	20.5 ± 0.3
(*Z*)-**5q**	4-OCH_3	69.0 ± 0.4	59.1 ± 1.9	50.3 ± 0.2	5.2 ± 1.0
(*E*)-**5q**	4-OCH_3	53.6 ± 0.8	47.8 ± 0.8	43.2 ± 0.8	9.5 ± 0.8
Hymexazol	/	49.4 ± 1.5	43.8 ± 1.4	58.0 ± 1.8	33.5 ± 1.1
Carbendazim	/	100 ± 0.0	100 ± 0.0	4.4 ± 0.5	70.1 ± 0.6
Tebuconazole	/	98.9 ± 0.3	99.5 ± 0.3	100 ± 0.0	100 ± 0.0

20%	40%	60%	80%	100%

Inhibition effect (%)

inhibitory rates of compounds (*Z*)-**5a**, (*Z*)-**5c**, (*Z*)-**5d**, (*Z*)-**5f**, (*Z*)-**5g**, (*Z*)-**5i**–(*Z*)-**5l**, (*Z*)-**5n**, (*Z*)-**5o**, (*E*)-**5e**–(*E*)-**5h**, and (*E*)-**5j**–(*E*)-**5p** reached above 80%, especially the rate of compound (*Z*)-**5o** was as high as 90.9%. Secondly, the target compounds also showed obvious bioactivity against *F. graminearum* with the inhibitory rates of 45.3–89.1%, which were higher than that of hymexazol (43.8%). In particular, the compounds (*E*)-**5g**, (*E*)-**5h**, (*E*)-**5k**, (*E*)-**5m**, and (*E*)-**5p** exhibited high inhibitory rates of 73.8%, 72.4%, 73.0%, 76.8%, and 89.1%, respectively. Moreover, there are eight compounds showing good activity with the inhibitory rates over 60% against *B. cinerea*. As the best of

them, the compound (*E*)-**5p** exhibited the inhibition rate of 71.9% to this fungus.

On the basis of the above bioassay results of inhibition rates, the EC$_{50}$ values of the target compounds against *R. solani* and *F. graminearum* were determined for further evaluating the antifungal activity in vitro. As recorded in Table 2, the target compounds showed better bioactivity against *R. solani* than *F. graminearum*, which was consistent with the inhibition rate data described above. The EC$_{50}$ values (0.41–29.51 µg/mL) of all the target compounds were more admiring than that of the control drug hymexazol (47.94 µg/mL), four compounds (*Z*)-**5g**, (*Z*)-**5k**, (*Z*)-**5o**,

Table 2 EC$_{50}$ values (µg/mL) of target compounds against *R. solani*

Compound	*R. solani*				*F. graminearum*			
	Regression equation	r	EC$_{50}$	95% CI	Regression equation	r	EC$_{50}$	95% CI
(*Z*)-**5a**	$y = 1.24x + 3.55$	0.97	14.82	11.19–19.63	$y = 0.54x + 4.28$	0.99	21.41	18.28–25.07
(*E*)-**5a**	$y = 1.09x + 3.41$	0.97	28.87	21.19–39.34	$y = 0.61x + 3.97$	0.96	49.78	30.89–80.24
(*Z*)-**5b**	$y = 1.25x + 3.42$	0.99	18.50	17.53–19.53	$y = 0.65x + 4.08$	0.99	25.58	23.53–27.81
(*E*)-**5b**	$y = 0.91x + 3.66$	0.94	29.51	19.15–45.48	$y = 0.83x + 3.68$	0.99	38.47	34.59–42.80
(*Z*)-**5c**	$y = 1.61x + 3.11$	0.99	14.84	14.22–15.49	$y = 0.74x + 4.05$	0.99	19.16	18.39–19.96
(*E*)-**5c**	$y = 1.52x + 3.01$	0.99	20.66	19.90–21.45	$y = 0.99x + 3.61$	0.99	25.74	21.46–30.88
(*Z*)-**5d**	$y = 1.23x + 3.62$	0.99	13.14	12.52–13.78	$y = 0.91x + 3.86$	0.99	17.59	16.67–18.57
(*E*)-**5d**	$y = 1.40x + 3.40$	0.99	14.04	12.40–15.91	$y = 0.63x + 3.91$	0.95	55.48	30.30–101.61
(*Z*)-**5e**	$y = 1.54x + 3.33$	0.96	12.20	8.75–16.99	$y = 0.56x + 4.51$	0.99	7.55	5.79–9.85
(*E*)-**5e**	$y = 1.30x + 3.60$	0.99	11.98	10.32–13.90	$y = 0.50x + 4.11$	0.99	60.71	48.29–76.33
(*Z*)-**5f**	$y = 0.87x + 4.28$	0.99	6.80	5.43–8.52	$y = 0.42x + 4.48$	0.98	18.99	14.94–24.14
(*E*)-**5f**	$y = 1.21x + 3.77$	0.99	10.29	8.56–12.37	$y = 0.49x + 4.17$	0.98	19.10	34.54–69.82
(*Z*)-**5g**	$y = 0.60x + 5.06$	0.96	0.80	0.49–1.32	$y = 0.53x + 4.29$	0.99	21.86	20.61–23.19
(*E*)-**5g**	$y = 1.24x + 3.55$	0.98	9.23	7.11–11.97	$y = 0.56x + 4.33$	0.99	15.96	13.59–18.76
(*Z*)-**5h**	$y = 0.97x + 4.06$	0.99	3.04	2.57–3.61	$y = 0.21x + 4.75$	0.98	14.85	11.84–18.63
(*E*)-**5h**	$y = 0.95x + 4.56$	0.97	2.89	2.18–3.84	$y = 0.35x + 4.65$	0.96	10.21	6.89–15.14
(*Z*)-**5i**	$y = 0.57x + 4.50$	0.99	7.55	6.71–8.50	$y = 0.62x + 4.18$	0.99	21.62	18.52–25.24
(*E*)-**5i**	$y = 0.74x + 4.30$	0.99	8.78	7.22–10.66	$y = 0.70x + 4.11$	0.99	18.70	16.07–21.78
(*Z*)-**5j**	$y = 0.64x + 4.62$	0.98	3.96	3.17–4.95	$y = 0.46x + 4.26$	0.98	40.36	28.58–57.01
(*E*)-**5j**	$y = 0.58x + 4.46$	0.98	8.49	6.10–11.82	$y = 0.45x + 4.16$	0.99	69.55	55.84–86.64
(*Z*)-**5k**	$y = 0.58x + 4.98$	0.99	1.08	0.89–1.30	$y = 0.50x + 4.50$	0.99	10.16	8.79–11.75
(*E*)-**5k**	$y = 1.01x + 4.12$	0.99	7.52	6.43–8.80	$y = 0.91x + 3.88$	0.99	16.99	14.96–19.31
(*Z*)-**5l**	$y = 0.76x + 4.47$	0.98	5.07	3.77–6.81	$y = 0.50x + 4.49$	0.98	10.32	8.08–13.19
(*E*)-**5l**	$y = 0.77x + 4.37$	0.99	6.56	5.33–8.07	$y = 0.71x + 3.91$	0.99	33.11	27.84–39.39
(*E*)-**5m**	$y = 2.31x + 2.59$	0.96	11.07	8.24–14.87	$y = 0.59x + 4.44$	0.98	8.71	6.00–12.64
(*Z*)-**5n**	$y = 0.64x + 4.71$	0.99	2.81	2.41–3.27	$y = 0.46x + 4.39$	0.99	20.81	17.22–25.17
(*E*)-**5n**	$y = 1.08x + 4.01$	0.99	8.15	6.58–10.11	$y = 0.61x + 3.92$	0.99	57.70	48.01–69.35
(*Z*)-**5o**	$y = 0.57x + 5.22$	0.99	0.41	0.29–0.57	$y = 0.63x + 4.39$	0.97	9.24	6.53–13.11
(*E*)-**5o**	$y = 0.74x + 4.96$	0.99	1.12	1.01–1.23	$y = 0.49x + 4.11$	0.98	65.96	43.65–99.68
(*E*)-**5p**	$y = 1.56x + 3.77$	0.99	6.19	5.74–6.67	$y = 0.83x + 4.27$	0.96	7.59	4.78–12.06
(*Z*)-**5q**	$y = 0.90x + 3.82$	0.94	20.31	13.57–30.41	$y = 0.57x + 4.26$	0.97	19.40	15.00–25.11
(*E*)-**5q**	$y = 1.93x + 2.21$	0.99	27.67	25.32–30.23	$y = 0.27x + 4.56$	0.97	41.36	27.63–61.95
Hymexazol	$y = 0.57x + 4.05$	0.95	47.94	27.12–84.74	$y = 1.70x + 2.17$	0.98	46.09	33.34–63.72
Carbendazim	$y = 8.35x + 7.19$	0.98	0.55	0.49–0.61	$y = 3.12x + 6.15$	0.98	0.43	0.28–0.67
Tebuconazole	$y = 5.25x + 0.85$	0.94	0.51	− 0.76–0.17	$y = 5.80x + 1.19$	0.99	0.21	− 0.88–1.39

Fig. 4 Inhibitory effect photographs of target compounds (*Z*)-**5o** (**A**) and (*E*)-**5o** (**B**) against *R. solani*
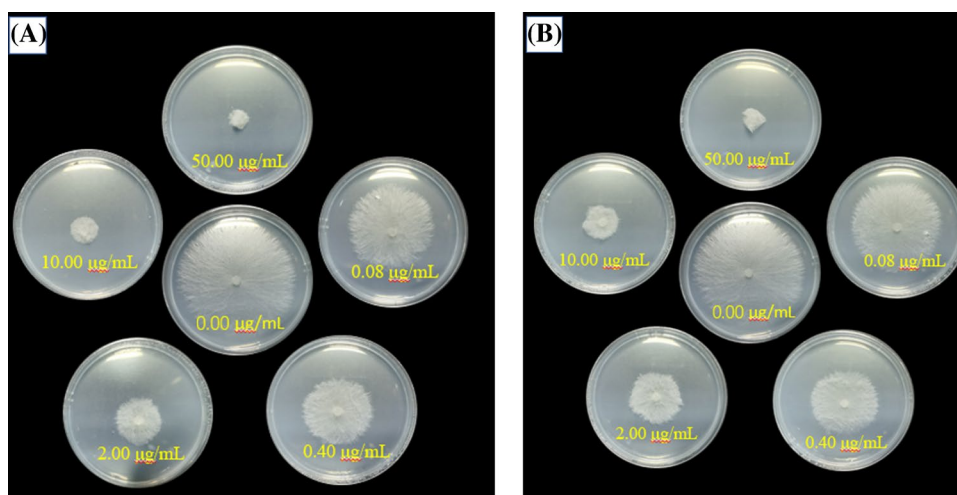
and (*E*)-**5o** of which presented very efficient bioactivity with the EC_{50} values of 0.80, 1.08, 0.41, and 1.12 μg/mL, respectively. Strikingly, the anti-*R. solani* activity of compound (*Z*)-**5o** was even slightly better than that of the common fungicides carbendazim ($EC_{50} = 0.55$ μg/mL) and tebuconazole ($EC_{50} = 0.51$ μg/mL). The inhibitory effect photographs of target compounds (*Z*)-**5o** and (*E*)-**5o** against *R. solani* were, respectively, illustrated in Fig. 4A, B. As for the EC_{50} values against *F. graminearum*, all the target compounds except (*E*)-**5a**, (*E*)-**5d**, (*E*)-**5e**, (*E*)-**5j**, and (*E*)-**5n** showed better bioactivity data (7.59–41.36 μg/mL) than hymexazol (46.09 μg/mL). Also noteworthy, there were four compounds (*Z*)-**5e**, (*E*)-**5m**, (*Z*)-**5o**, and (*E*)-**5p** exhibiting appreciable the EC_{50} values below 10 μg/mL.

Structure–activity relationship (SAR) analysis

According to the EC_{50} data against *R. solani* and *F. graminearum*, the structure–activity relationship (SAR) of the target compounds was analyzed to conclude following two important rules. The first is that the antifungal activity of (*Z*)-isomers was generally better than that of (*E*)-isomers. Apart from the (*Z*)-isomers of **5e** and **5h**, and the (*E*)-isomers of **5e**, **5h**, **5m**, and **5p**, all the other (*Z*)-isomers displayed more preferable EC_{50} values than the corresponding (*E*)-isomers. For an example, the different isomers (*Z*)-**5o** and (*E*)-**5o**, respectively, presented the EC_{50} values of 0.41 and 1.12 μg/mL against *R. solani*, and 9.24 and 65.96 μg/mL against *F. graminearum*. The second conclusion is that different substituents at the benzene ring showed significant effects on the antifungal activity. When the benzene ring contains the bulky electron absorbing groups, such as Cl, Br or CF_3, it is helpful to improve the antifungal activity. In particular, when any of the three groups was introduced to the 4-position of the benzene ring, the corresponding compounds showed perfect antifungal activity, which is particularly obvious in

the inhibition against *R. solani*. For example, this is the case with the compounds (*Z*)-**5g** and (*E*)-**5g** ($R^1 = 4$-Cl, anti-*R. solani* $EC_{50} = 0.80$ and 9.23 μg/mL, respectively), (*Z*)-**5k** and (*E*)-**5k** ($R^1 = 4$-Br, anti-*R. solani* $EC_{50} = 1.08$ and 7.52 μg/mL, respectively), and (*Z*)-**5o** and (*E*)-**5o** ($R^1 = 4$-CF_3, anti-*R. solani* $EC_{50} = 0.41$ and 1.12 μg/mL, respectively).

In vivo anti-*R. solani* activity of compound (Z)-5o

Encouraged by the in vitro bioassay result, the in vivo preventative effect experiment of the highly bioactive compound (*Z*)-**5o** was conducted for further evaluating the practical application value as a potential DMI fungicide. The commonly used fungicide validamycin and representative DMI fungicide tebuconazole were selected as the positive controls. The in vivo bioassay results against *R. solani* inoculated on rice leaves were vividly illustrated in Fig. 5. From Fig. 5, it can be seen that the compound (*Z*)-**5o** at 200 μg/mL showed excellent bioactivity in vivo, with the preventative efficacy of 94.50%, which was very close to that of tebuconazole (96.33%). When the concentration of (*Z*)-**5o** was diluted to 100 μg/mL, its bioactivity remained at 50.27%, which was significantly higher than that of tebuconazole (30.19%). This in vivo bioassay result implies the rationality of the molecular design of the target compounds represented by compound (*Z*)-**5o**. At the same time, as a new class of DMI lead molecules, the 1,2,4-triazole derivatives containing the oxime ether and cyclohexyl fragments have the potential to further optimize the structures for improving their antifungal activity.

Effect on hyphae morphology of compound (Z)-5o

The scanning electron microscopy (SEM) was used to investigate the mycelium morphology of *R. solani*

Fig. 5 In vivo preventative effect of compound (*Z*)-**5o** against *R. solani* at 200 μg/mL on rice leaves

Compound	Preventative efficacy (100 μg/mL)
(*Z*)-**5o**	50.27%
Tebuconazole	31.19%
Validamycin	98.11%
CK (0.5% DMSO)	/

Compound	Preventative efficacy (200 μg/mL)
(*Z*)-**5o**	94.50%
Tebuconazole	96.33%
Validamycin	100%
CK (0.5% DMSO)	/
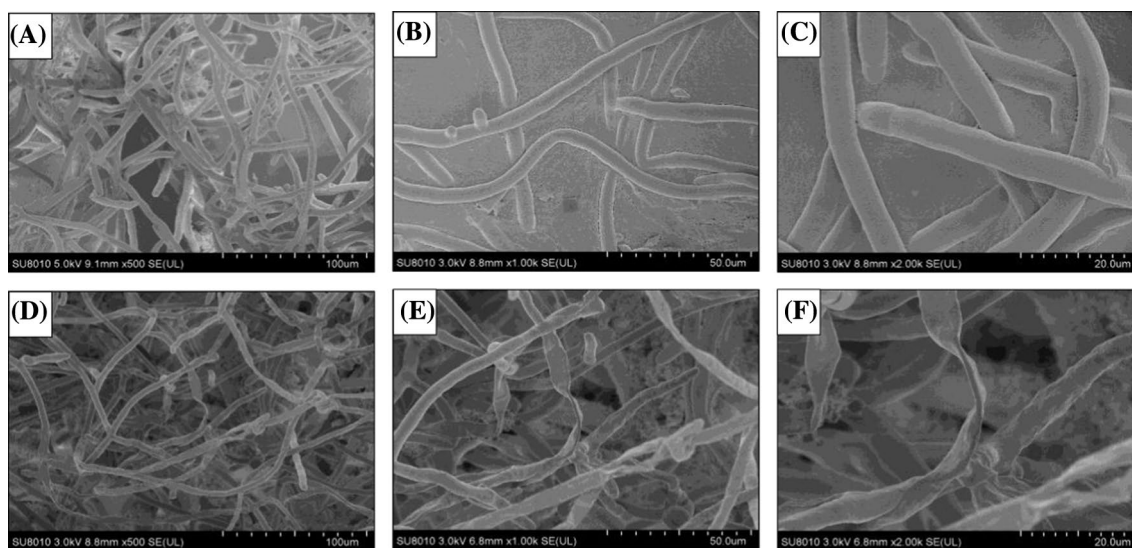
Fig. 6 SEM images of mycelium morphology. **A–C**: Blank controls; **D–F**: Treatments with (*Z*)-**5o** at 50 μg/mL

influenced by compound (*Z*)-**5o** at 50 μg/mL and meanwhile, the equivalent solvent DMSO was used as the blank control. As the SEM images shown in Fig. 6A–C, the mycelia treated with DMSO was normal, their appearances were plump and their surfaces were smooth. On the contrary, after the mycelia was treated with the compound (*Z*)-**5o**, they became abnormal, their appearances looked wizened and their surfaces seemed wrinkled (Fig. 6D–F).

This phenomenon indicated that the compound (*Z*)-**5o**, like other traditional triazole fungicides, can inhibit mycelial growth by inhibiting ergosterol biosynthesis to affect the normal function of cell membrane.

Molecular docking comparison of isomers (*Z*)-5o and (*E*)-5o with RsCYP51

The (*Z*)-isomer and (*E*)-isomer of a same compound usually show different degrees of antimicrobial activity, but there are few reports on the mechanism leading to this difference of bioactivity [35–37]. Molecular docking study not only provides an insight between ligand and macromolecules in binding location, but also confirms the experimental observations to a certain degree [38]. In the present work, the molecular design focused on ergosterol biosynthesis inhibitions (DMIs) strikingly resulted in the discovery of promising candidate (*Z*)-**5o** that presented the conspicuous inhibitory effect against *R. solani* in vitro and in vivo. However, its corresponding isomer (*E*)-**5o** showed lower antifungal activity, whether against *R. solani* or *F. graminearum*. Thereupon, the binding modes of the both isomers (*Z*)-**5o** and (*E*)-**5o** with *Rs*CYP51 were, respectively, analyzed to preliminarily

explore the molecular mechanism leading to differences in antifungal activity by molecular docking method.

The homology model of *Rs*CYP51 was built by Swiss-model online website at the beginning process. The constructed homology models were verified the reliability by Pymol and found it possessed the best alignment with the template. The Ramachandran plot and RMSD values were 87.42% and 0.137, respectively. The molecular docking results revealed that the binding energies of (*Z*)-**5o** and (*E*)-**5o** were separately − 8.55 and − 6.76 kJ/ mol. The lower binding energy meant that (*Z*)-**5o** bound more closely to the target protein, which is consistent with its higher antifungal activity. Furthermore, the molecular docking diagrams of target compounds (*Z*)-**5o** and (*E*)-**5o** with *Rs*CYP51 are illustrated in Fig. 7A–C and D, F, respectively. There are 17 interactions between compound (*Z*)-**5o** and surrounding amino acid residues with bond length less than 5 Å (Fig. 7C), compared only 11 interactions of (*E*)-**5o** (Fig. 7F). Both ligand molecules interacted with amino acids mainly through 1,2,4-triazole ring, cyclohexyl group, benzene ring and trifluoromethyl connected at 4-position of benzene ring. The interactions between triazole ring and residues in the two molecules included the key coordination between the 4-position
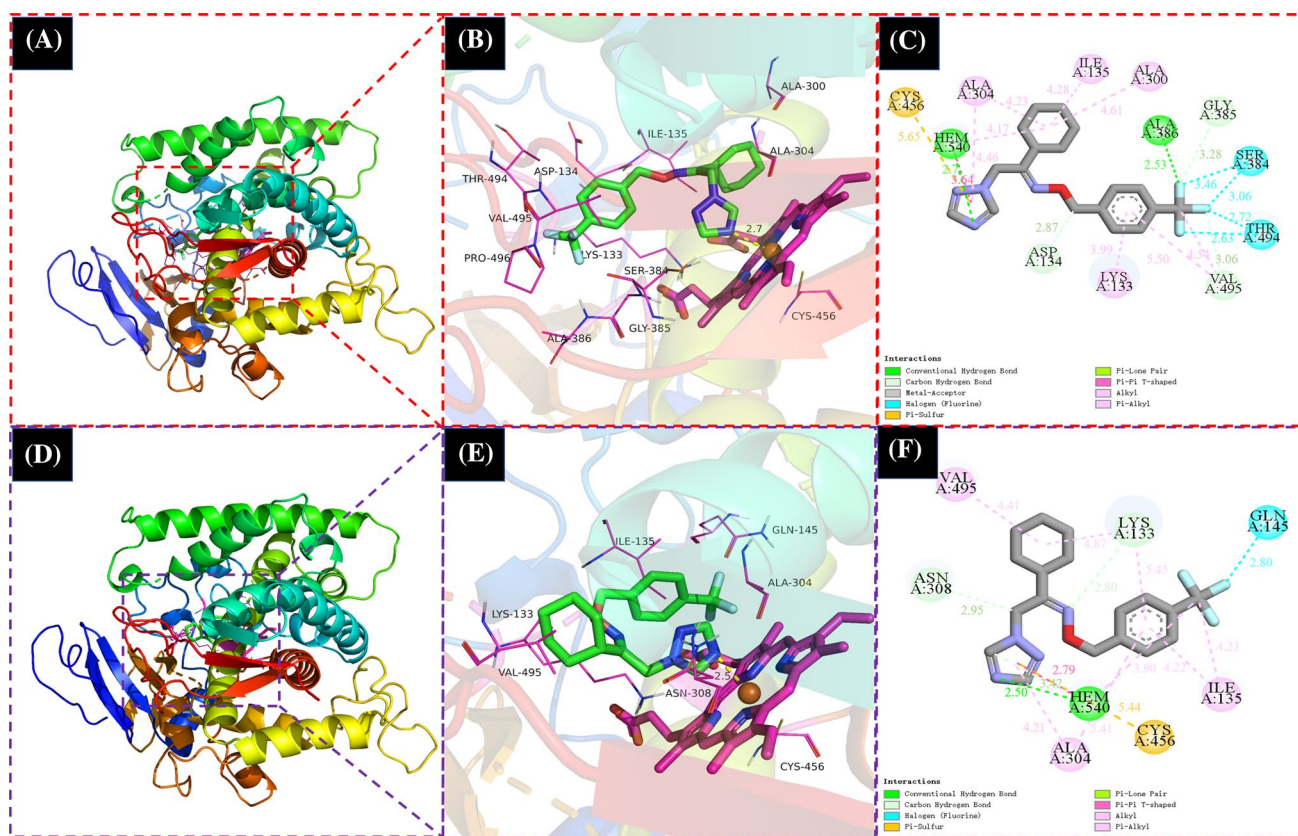

Fig. 7 Molecular docking modes of target compounds (*Z*)-**5o** (**A–C**) and (*E*)-**5o** (**D–F**) with *Rs*CYP51

nitrogen atom of triazole and the iron ion in porphyrin heme (HEM), the π–π stacking interaction of triazole ring with HEM, and the σ–π stacking interaction of triazole ring with alanine (ALA A:304), which reflected that the two isomers (Z)-**5o** and (E)-**5o** have a similar mode of action with the target protein. However, the interactions between trifluoromethyl and surrounding amino acid residues were significantly different between the two isomers. For (Z)-**5o**, the three fluorine atoms of its trifluoromethyl formed seven different types of hydrogen bonds with glycine (GLY A:385), alanine (ALA A:386), serine (SER A:384) and threonine (THR A:494), respectively (Fig. 7C). In contrast, (E)-**5o** only formed only one hydrogen bond with glutamine (GLN A:145) (Fig. 7F). The strong hydrogen bond interactions between (Z)-**5o** and the amino acid residues of the target protein led to its low binding energy, which may be the main reason why its antifungal activity was higher than that of (E)-**5o**.

Conclusions

For the purpose of screening new ergosterol biosynthesis inhibitors (DMIs), a series of triazole derivatives containing the oxime ether bridge group were designed, synthesized and characterized by ^{1}H NMR, ^{13}C NMR, ^{19}F NMR, HRMS and X-ray diffraction analyses. The bioassay results indicated that the target compounds possessed good antifungal activity against *R. solani*, *F. graminearum* and *B. cinerea*. The (Z)- and (E)-isomers of target compounds were successfully separated, and most of the (Z)-isomers showed higher antifungal activity than the corresponding (E)-isomers. As a most promising target compound, (Z)-**5o** was found possessing excellent antifungal activity against *R. solani* with the EC$_{50}$ value of 0.41 μg/mL in vitro and preventive effect of 94.58% in vivo at 200 μg/mL, which was even comparable to the common commercialized fungicide tebuconazole. The compound (Z)-**5o** could significantly inhibit mycelial growth by destroying mycelial cell membrane. By comparing the molecular docking modes of (Z)-**5o** and (E)-**5o** with the potential target protein *Rs*CYP51, it was preliminarily clarified that (Z)-**5o** effectively reduced the binding energy through strong hydrogen bond interactions with the amino acid residues of the target protein and made its antifungal activity higher than compound (E)-**5o**.

Materials and methods

Instruments and chemicals

The solvents and reagents, used directly for synthesizing the target compounds, were purchased from commercial pathways (Nanjing Wanqing Glass Instrument Co. Ltd and Nanjing Lattice Chemical Technology Co. Ltd, etc.). An uncorrected Automatic Melting Point Apparatus (Staffordshire, UK) was selected to measure the melting point of solid compounds. The ^{1}H NMR, ^{13}C NMR, and ^{19}F NMR were recorded on a 400 MHz NMR spectrometer ((Bruker, Germany) with CDCl$_3$ as the solvent and TMS (tetramethylsilane) as the internal standard. Data for $[M + H]^+$ values were collected on a Triple TOF 5600 Plus LC/MS/MS spectrometer (AB Sciex, America). Thin-layer chromatography (Yuhua, China) and ultraviolet detector (UV, 254 nm) were chosen to monitor the whole synthetic stage. Ultrastructure of fungal mycelium was observed by a SU8018 scanning electron microscope (Hitachi, Japan).

Synthesis procedures for intermediates 2–4

The starting material 1-cyclohexylethan-1-one **1** (1.5 g, 11.9 mmol) dissolved in acetonitrile (20 mL) was firstly added into a 50 mL three-necked flask. Then, *N*-bromosuccinimide (NBS) (4.2 g, 23.7 mmol) and the initiator trimethylsilyl trifluoromethanesulfonate (TMS·OTf) (0.13 g, 0.6 mmol) was successively added. After the mixed solution was stirred at room temperature for 24 h, the solvent was removed by decompressive distillation. The residue was extracted three times with dichloromethane (20 mL × 3). The organic phases were combined, dried with anhydrous sodium sulfate, filtered and concentrated on vacuum to obtain a yellow oil, namely 2-bromo-1-cyclohexylethan-1-one **2**, in yield of 88%.

The compound **2** (1.67 g, 8.15 mmol) was dissolved in 5 mL of acetonitrile and added dropwise to the acetonitrile solution (20 mL) containing sodium 1,2,4-triazole (0.89 g, 9.77 mmol). After heating and refluxing for 5 h, the reaction solution was concentrated under reduced pressure. The resulting mixture was extracted with dichloromethane for three times (20 mL × 3). The organic phases were combined, dried, filtered and followed by the removal of acetonitrile under vacuum to obtain a yellow light oily liquid named 1-cyclohexyl-2-(1*H*-1,2,4-triazol-1-yl)ethan-1-one **3** in yield of 78%.

The compound **3** (1.28 g, 6.6 mmol) and potassium carbonate (1.37 g, 9. 9 mmol) were successively added to a 50 mL three-necked flask under ice bath. Hydroxylamine hydrochloride (0.92 g, 13.2 mmol) dissolved in 6 mL of water was added dropwise to the above reaction solution.

The obtained mixture was then heated and refluxed for 6 h. After concentrating under reduced pressure, the residue was added into 10 mL of ice water, precipitated and filtered to give a white solid with a yield of 75%, that is 1-cyclohexyl-2-(1*H*-1,2,4-triazol-1-yl)ethan-1-one oxime **4.**

Synthesis procedures for target compounds and separation of (*Z*)/(*E*)-isomers

The intermediate **4** (0.5 g, 2.4 mmol) was dissolved in 20 mL of *N*,*N*-dimethyl formamide (DMF), and 60% NaH (0.12 g, 2.9 mmol) dissolved in 5 mL DMF was then added slowly dropwise. After the mixture was stirred for 0.5 h in an ice bath, the various of substituted benzyl chloride (2.9 mmol) was added dropwise. The reaction solution was continuously stirred in an ice bath for 1 h, and then in room temperature for 4 h. The organic phase was extracted three times by ethyl acetate (20 mL × 3), washed twice in turn with saturated sodium bicarbonate and salt water, dried over anhydrous sodium sulfate, filtered and concentrated under low pressure to obtain the 1,2,4-triazole derivatives containing the oxime ether moiety **5a**–**5q**. The (*Z*)/(*E*)-isomers were separated and purified one by one by silica gel column chromatography (isopropanol + petroleum ether, V:V = 1:16) to present the desired target compounds (*Z*)-**5a**–(*Z*)-**5l**, (*Z*)-**5n**, (*Z*)-**5o**, (*Z*)-**5q** and (*E*)-**5a**–(*E*)-**5q**.

Antifungal bioassay of target compounds in vitro and in vivo

The mycelium growth inhibition method was used to test the in vitro antifungal potential of target compounds against four important agricultural pathogenic fungi, *R. solani*, *F. graminearum*, *B. cinerea* and *A. solani* [39–41]. Three commercialized pesticides were selected as the positive control, including hymexazol, carbendazim and tebuconazole, which are usually applied to control one or more plant diseases caused by above plant pathogenic fungi [42–44]. The dimethylsulfoxide (DMSO) solution (100 μL) containing different concentrations of the test compounds was first added in 45 mL of potato dextrose agar (PDA) medium. After shaking completely well, the medium was equally poured into three nine-centimeter petri plates. Meanwhile, three above-mentioned positive controls and blank control which containing same amount of DMSO were elaborately set. After the mediums were solidified, the mycelium dishes with a diameter of 5 mm were inoculated onto the medium centers and cultivated for 2–6 days at 25 ± 1 °C in dark environment. When the colony diameter of the blank control reached about 70 mm, the colony diameters of different treatments were measured to calculate the inhibition rates of test compounds.

Subsequently, the inhibition rates of the target compounds against *R. solani* and *F. graminearum* at five appropriate concentrations were determined, which were used to establish the regression equations and calculate the respective EC_{50} values.

The compound (*Z*)-**5o** with the best antifungal activity against *R. solani* was further tested the antifungal activity in vivo using detached rice leaf assay [45]. The fresh rice leaves were cut to 10 cm long segments and maintained the leaves moist until use. The compound (*Z*)-**5o** and positive control tebuconazole were dissolved in proper amount of DMSO and diluted using 0.05% Tween-80 to obtain the 200 μg/mL solutions. The equal amount of DMSO was served as the blank control. After the prepared solutions were sprayed on the surface of the rice leaves for 24 h, the 5 mm mycelium disks of *R. solani* were inoculated onto the leaf center with 15 repetitions. The treatments were cultivated at 25 ± 1 °C under the 12 h-light and 12 h-dark cycle condition. When the disease spots basically spread throughout the rice leaves, the lengths of the lesion were measured to calculate the preventative efficacies.

SEM study

The fungus *R. solani* was cultivated on PDA medium containing 50 μg/mL of compound (*Z*)-**5o** and on the medium containing the same amount of solvent DMSO as the blank control. When the mycelium of the blank control grew to half of the medium diameter, the 5 mm long and 2 mm wide mycelium blocks were cut from the edge of colony. The samples treated by the previously reported method were observed with the scanning electron microscopy (SEM) [46].

Molecular docking study

The three-dimensional structures of compounds (*Z*)-**5o** and (*E*)-**5o** were drawn and optimized by SYBYL 2.0 software (Shanghai Tri-I. Biotech. Inc., China). Swiss-model online software (https://swissmodel.expasy.org/) was used to rebuilt the three-dimensional structures of *Rs*CYP51 (CYP51 from *R. solani*). The template protein (PDB code: 4UHL) and *Rs*CYP51 protein sequence were downloaded from the RCSB protein database (https://www.rcsb.org/) and Uniport (https://www.uniprot.org), respectively. The molecular docking was completed by the AutoDock 4.2.6. Pymol 1.7.6 was used to handle the docking results, conduct the alignment of 4UHL, and constructed protein. And Discovery studio 4.5 was used to calculate the binding energies and generate the docking resulting figures.

Appendix A

The physical and spectroscopic data, crystal structure information and molecular docking related information of target compounds are provided in the Supporting Information. The copies of corresponding [1] H NMR, ^{13}C NMR, ^{19}F NMR, and HRMS spectrograms are also presented in the Supporting Information.

Declarations

Conflicts of interest The authors declare that they have no conflict of interest.

References

1. Wang Q, Tang B-H, Cao M-H (2020) Synthesis, characterization, and fungicidal activity of novel fangchinoline derivatives. Bioorg Med Chem 28:115778. https://doi.org/10.1016/j.bmc.2020.115778

2. Sheng T, Kong M-M, Wang Y-J, Wu H-J, Gu Q, Chuang AS, Li S-K, Gao X-W (2021) Discovery and preliminary mechanism of 1-carbamoyl β-carbolines as new antifungal candidates. Eur J Med Chem 222:113563. https://doi.org/10.1016/j.ejmech.2021.113563

3. Aggarwal R, Sumran G (2020) An insight on medicinal attributes of 1,2,4-triazoles. Eur J Med Chem 205:112652. https://doi.org/10.1016/j.ejmech.2020.112652

4. Xu H, Su X, Guo M-B, An R, Mou Y-H, Zhuang H, Guo C (2020) Design, synthesis, and biological evaluation of novel miconazole analogues containing selenium as potent antifungal agents. Eur J Med Chem 198:112360. https://doi.org/10.1016/j.ejmech.2020.112360

5. Foley DA, Callaghan YO, Brien NMO, Carthy FOM, Maguire AR (2010) Synthesis and characterization of stigmasterol oxidation products. J Agric Food Chem 58:1165–1173. https://doi.org/10.1021/jf9024745

6. Zhang J-X, Li L-P, Lv Q-Z, Yan L, Wang Y, Jiang Y-Y (2019) The Fungal CYP51s: Their functions, structures, related drug resistance, and inhibitors. Front Microbiol 10:691. https://doi.org/10.3389/fmicb.2019.00691

7. Price CL, Parker JE, Warrilow AG, Kelly DE, Kelly SL (2015) Azole fungicides–understanding resistance mechanisms in agricultural fungal pathogens. Pest Manag Sci 71:1054–1058. https://doi.org/10.1002/ps.4029

8. Tyndall JDA, Sabherwal M, Sagatova AA, Keniya MV, Negroni J, Wilson RK, Woods MA, Tietjen K, Monk BC (2016) Structural and functional elucidation of yeast lanosterol 14α-demethylase in complex with agrochemical antifungals. PLoS ONE 1(12):e0167485. https://doi.org/10.1371/journal.pone.0167485

9. Fan X-Y, Fu Y, Nie Y-X, Matsumoto H, Wang Y, Hu T-T, Pan Q-Q, Lv T-X, Fang H-D, Xu H-R, Wang Y, Ge H, Zhu G-N, Liu Y-H, Wang Q-W, Wang M-C (2021) Keystone taxa-mediated bacteriome response shapes the resilience of the paddy ecosystem to fungicide triadimefon contamination. J Hazard Mater 417:126061. https://doi.org/10.1016/j.jhazmat.2021.126061

10. Macar TK, Macar O, Yalçın M, Yalçın E, Çavuşoğlu K (2021) Preventive efficiency of Cornelian cherry (*Cornus mas* L.) fruit extract in diniconazole fungicide-treated *Allium cepa* L. roots. Sci Rep 11:2534. https://doi.org/10.1038/s41598-021-82132-4

11. Cui N, Xu H-Y, Yao S-J, He Y-W, Zhang H-C, Yu Y-L (2018) Chiral triazole fungicide tebuconazole: enantioselective bioaccumulation, bioactivity, acute toxicity, and dissipation in soils. Environ Sci Pollut Res 25:25468–25475. https://doi.org/10.1007/s11356-018-2587-9

12. Wang Y, Wang M-M, Xu L-T, Sun Y, Feng J-T (2020) Baseline sensitivity and toxic action of the sterol demethylation inhibitor flusilazole against botrytis cinerea. Plant Dis 104:2986–2993. https://doi.org/10.1094/PDIS-11-19-2478-RE

13. Mısır MN, Mısır G, Bekircan O, Kantekin H, Oztürk D, Durmus M (2021) Sulfur bridged new metal-free and metallo phthalocyanines carrying 1,2,4-triazole rings and their photophysicochemical properties. Polyhedron 207:115361. https://doi.org/10.1016/j.poly.2021.115361

14. Zhang Y, Damu GLV, Cui S-F, Mi J-L, Tangadanchu VKR, Zhou C-H (2017) Discovery of potential antifungal triazoles: design, synthesis, biological evaluation, and preliminary antifungal mechanism exploration. Med Chem Commun 8:1631. https://doi.org/10.1039/C7MD00112F

15. Su S-J, Chen M, Li Q, Wang Y-H, Chen S, Sun N, Xie C-W, Huai Z-Y, Huang Y-J, Xue W (2021) Novel penta-1,4-diene-3-one derivatives containing quinazoline and oxime ether fragments: design, synthesis and bioactivity. Bioorg Med Chem 32:115999. https://doi.org/10.1016/j.bmc.2021.115999

16. Han X, Lv W, Guo S-Y, Cushman M, Liang J-H (2015) Synthesis and structure–activity relationships of novel 9-oxime acylides with improved bactericidal activity. Bioorg Med Chem 23:6437–6453. https://doi.org/10.1016/j.bmc.2015.08.020

17. Koo SJ, Ahn SC, Lim JS, Chae SH, Kim JS, Lee JH, Cho JH (1997) Biological activity of the new herbicide LGC-40863 {benzophenone *O*-[2,6-bis[(4,6-dimethoxy-2-pyrimidinyl)oxy]benzoyl]oxime}. Pestic Sci 51:109–114. https://doi.org/10.1002/(SICI)1096-9063(199710)51:2<109::AID-PS585>3.0.CO;2-7

18. Bian Q, Zhao R-Q, Peng X-J, Gao L-J, Zhou G-N, Yu S-J, Zhao W-G (2021) Design, Synthesis, and fungicidal activities of novel piperidyl thiazole derivatives containing oxime ether or oxime ester moieties. J Agric Food Chem 69:3848–3858. https://doi.org/10.1021/acs.jafc.0c07581

19. Ouyang G, Cai X-J, Chen Z, Song B-A, Bhadury PS, Yang S, Jin L-H, Xue W, Hu D-Y, Song Z (2008) Synthesis and antiviral activities of pyrazole derivatives containing an oxime moiety. J Agric Food Chem 56:10160–10167. https://doi.org/10.1021/jf802489e

20. Fu C-R, Pei J, Ning Y, Liu M, Shan P-C, Liu J, Li Y-Q, Hu F-Z, Zhu Y-Q, Yang H-Z, Zou X-M (2014) Synthesis and insecticidal activities of novel pyrazole oxime ether derivatives with different substituted pyridyl rings. Pest Manag Sci 70:1207–1214. https://doi.org/10.1002/ps.3672

21. Tellier F, Fritz R, Kerhoas L, Ducrot P-H, Einhorn J, Sinclair AC, Leroux P (2008) Characterization of metabolites of fungicidal

cymoxanil in a sensitive strain of botrytis cinerea. J Agric Food Chem 56:8050–8057. https://doi.org/10.1021/jf8010917

22. Nofiani R, Mattos-Shipley KD, Lebe K, Han L-C, Iqbal Z, Willis C, Simpson T, Cox R (2018) Strobilurin biosynthesis in Basidiomycete fungi. Nat Commun 9:3940. https://doi.org/10.1038/s41467-018-06202-4

23. Takagaki M, Kataoka S, Kida K, Miura I, Fukumoto S, Tamai R (2010) Disease-controlling effect of a novel fungicide pyribencarb against *Botrytis cinerea*. J Pestic Sci 35(1):10–14. https://doi.org/10.1584/jpestics.G09-24

24. Ravenzwaay BV, Akiyama M, Landsiede R, Kieczka H, Cunha G, Schneider S, Kaspers U, Kaufmann W, Osawa M (2007) Toxicological overview of a novel strobilurin fungicide, orysastrobin. J Pestic Sci 32:207. https://doi.org/10.1584/jpestics.G06-52

25. Reuveni M (2000) Efficacy of trifloxystrobin (Flint), a new strobilurin fungicide, in controlling powdery mildews on apple, mango and nectarine, and rust on prune trees. Crop Prot 19:335–341. https://doi.org/10.1016/S0261-2194(00)00026-0

26. Wang M-L, Du Y, Ling C, Yang Z-K, Jiang B-B, Duan H-X, An J, Li X-H, Yang X-L (2021) Design, synthesis and antifungal/anti-oomycete activity of pyrazolyl oxime ethers as novel potential succinate dehydrogenase inhibitors. Pest Manag Sci. https://doi.org/10.1002/ps.6418

27. Blessing B, Submuth R (1993) Stimulating effects in bacterial toxicity tests—a source of error in evaluating the risk posed by chemicals. Wat Res 27:225–229. https://doi.org/10.1016/0043-1354(93)90079-W

28. European Food Safety Authority (EFSA), Parma I (2014) Conclusion on the peer review of the pesticide risk assessment of the active substance fenhexamid. EFSA J 12(7):3744. https://doi.org/10.2903/j.efsa.2014.3744

29. Peng J-N, Wang K, Feng T-Y, Zhang H-Z, Li X-H, Qi Z-Q (2020) The effect (1S,2R-((3-bromophenethyl)amino)-*N*-(4-chloro-2-trifluoromethylphenyl) cyclohexane-1-sulfonamide) on *Botrytis cinerea* through the membrane damage mechanism. Molecules 25(1):94. https://doi.org/10.3390/molecules25010094

30. Wang C, Li Z-L, Ju Y-M, Koo S (2012) Mechanism and scope of the MnIII-initiated oxidation of β-ketocarbonyl compounds: furan synthesis. Eur J Org Chem 35:6976–6985. https://doi.org/10.1002/ejoc.201201194

31. Liu X-W, Ma J-M, Colson A-O, Doersen DC, Ebetino FH (2008) Synthesis and biological activity of novel peptide mimetics as melanocortin receptor agonists. Bioorg Med Chem Lett 18:1223–1228. https://doi.org/10.1016/j.bmcl.2007.11.109

32. Chen M, Geng C-W, Han L, Liu Y, Yu Y-K, Lu A-M, Yang C-L, Li G-H (2021) Design, synthesis, crystal structure, and herbicidal activity of novel pyrrolidine-2,4-dione derivatives incorporating an alkyl ether pharmacophore with natural tetramic acids as lead compounds. New J Chem 45:5621. https://doi.org/10.1039/D1NJ00119A

33. Jiao J, Chen M, Sun S-X, Si W-J, Wang X-B, Ding W-J, Fu X-C, Wang A, Yang C-L (2021) Synthesis, bioactivity evaluation, 3D-QSAR, and molecular docking of novel pyrazole-4-carbohydrazides as potential fungicides targeting succinate dehydrogenase. Chin J Chem 39:323–329. https://doi.org/10.1002/cjoc.202000438

34. Wang X-B, Chai J-Q, Kong X-Y, Jin F, Chen M, Yang C-L (2021) Expedient discovery for novel antifungal leads: 1,3,4-oxadiazole derivatives bearing a quinazolin-4(3*H*)-one fragment. Bioorg Med Chem 45:116330. https://doi.org/10.1016/j.bmc.2021.116330

35. Mehan AS, Senturk E, Kara EM, Yusufoglu AS (2019) Synthesis, E/Z isomerization, and antimicrobial studies of different structured novel ketone derivatives. JOTCSA 6(2):177−188. https://doi.org/10.18596/jotcsa.486487

36. Jebli N, Arfaoui Y, Hecke KV, Cavalier JF, Touil S (2021) Experimental and computational investigation of Z/E isomerism, X-ray crystal structure and molecular docking study of (2-(hydroxyimino)cyclohexyl)diphenylphosphine sulfide, a potential antibacterial agent. J Mol Struc 1229:129634. https://doi.org/10.1016/j.molstruc.2020.129634

37. Emami S, Falahati M, Banifatemi A, Moshirl K, Shafiee A (2002) Stereoselective synthesis and in vitro antifungal evaluation of (E)- and (Z)-imidazolylchromanone oxime ethers. Arch Pharm Med Chem 7:318−324. https://doi.org/10.1002/1521-4184(200209)335:7<318::AID-ARDP318>3.0.CO;2-O

38. Bolel P, Mahapatra N, Datta S, Halder M (2013) Modulation of accessibility of subdomain IB in the pH-dependent nteriaction of bovine serum albumin with cochineal red A: a combined view from spectroscopy and docking simulations. J Agric Food Chem 61:4606–4613. https://doi.org/10.1021/jf305395n

39. Jeger MJ, Lamour A, Gilligan CA, Otten W (2008) A fungal growth model fitted to carbon-limited dynamics of *Rhizoctonia solani*. New Phytologist 178: 625–633. https://doi.org/10.1111/j.1469-8137.2008.02394.x

40. Dyer RB, D.Plattner R, F.kendra D, Brown DW (2005) *Fusarium graminearum* TRI14 is required for high virulence and DON productionon wheat but not for DON synthesis *in vitro*. J Agric Food Chem 53:9281−9287. https://doi.org/10.1021/jf051441a

41. Williamson B, Tudzynski B, Tudzynski P, Van Kan JAL (2017) Pathogen profile *Botrytis cinerea*: the cause of grey mould disease. Mol Plant Pathol 8(5):561–580. https://doi.org/10.1111/j.1364-3703.2007.00417.x

42. Diao X, Han Y-Y, Liu C-L (2018) The fungicidal activity of tebuconazole enantiomers against *Fusarium graminearum* and its selective effecton DON production under different conditions. J Agric Food Chem 66:3637–3643. https://doi.org/10.1021/acs.jafc.7b05483

43. Fan L-L, Luo Z-F, Yang C-F, Guo B, Miao J, Chen Y (2021) Design and synthesis of small molecular 2-aminobenzoxazoles as potential antifungal agents against phytopathogenic fungi. Mol Divers. https://doi.org/10.1007/s11030-021-10213-7

44. Liu S-M, Chen Y, Yu J-J, Chen C-J, Wang Z-X, Zhou M-G (2010) Transfer of the beta-tubulin gene of *botrytis cinerea* with resistance to carbendazim into *Fusarium graminearum*. Pest Manag Sci 66(5):482–489. https://doi.org/10.1002/ps.1897

45. Zhang Z-J, Zeng Y, jiang Z-Y, Shu B-S, Sethuraman V, Zhong G-H (2018) Design, synthesis, fungicidal property and QSAR studies of novel β-carbolines containing urea, benzoylthiourea and benzoylurea for the control of rices heath blight. Pest Manag Sci 74:1736–1746. https://doi.org/10.1002/ps.4873

46. Yan X-J, Liang X-M, Jin S-H, Lv J-P, Yu C-X, Qin W-Y, Li B-J, Yuan H-J, Qi S-H, Shi Y-X, Wu J-P, Chen F-H, Wang D-Q (2010) Primary study on mode of action for macrocyclic fungicide candidates (7B3, D1) against *Rhizoctonia solani* Kuhn. J Agric Food Chem 58:2726–2729. https://doi.org/10.1021/jf9037369